# Plasma interferometry and how the bound-electron contribution can bend fringes in unexpected ways

Joseph Nilsen and Walter R. Johnson

Utilizing a new average atom code, we calculate the index of refraction in C, Al, Ti, and Pd plasmas and show many conditions over which the bound-electron contribution dominates the free electrons as we explore photon energies from the optical to 100 eV (12 nm) soft x rays. For decades measurement of the electron density in plasmas by interferometers has relied on the approximation that the index of refraction in a plasma is due solely to the free electrons and therefore is less than 1. Recent measurements of Al plasmas using x-ray laser interferometers observed fringes bending in the opposite direction than expected due to the bound-electron contribution causing the index of refraction to be larger than 1. During the next decade x-ray free-electron lasers and other sources will be available to probe a wider variety of plasmas at higher densities and shorter wavelengths, so understanding the index of refraction in plasmas is essential. 

*OCIS codes:* 340.7450, 120.3180, 120.5710, 140.7240.

## 1. Introduction

Optical interferometers have been used for many decades to measure the electron density of plasmas.[1] The basic assumption in the data analysis is that the index of refraction of a plasma can be calculated from the free-electron density.[1,2] This implies that the number of fringe shifts in the interferometer is directly proportional to the electron density of the plasma. This also makes the index of refraction in the plasma less than 1. When x-ray lasers became available, the same assumptions were used as the interferometer was extended to shorter wavelengths to probe even higher-density plasmas. The first x-ray laser interferometer[3] was demonstrated about 10 years ago using the 15.5 nm Ne-like Y laser at the Nova facility at Lawrence Livermore National Laboratory (LLNL). Since then, many x-ray laser interferometers,[4–6] and a high-order harmonic interferometer,[7] have been used in the wavelength range of 14–72 nm. This covers photon energies from 17 to 89 eV.

Experiments recently conducted at the Advanced Photon Research Center at the Japan Atomic Energy Research Institute (JAERI) using the 13.9 nm Ni-like Ag laser,[4] and at the Compact Multipulse Terawatt (COMET) laser facility at LLNL using the 14.7 nm Ni-like Pd laser,[5] observed anomalous behavior of fringe lines in interferometer experiments of Al plasmas where the fringe lines bent in the opposite direction than was expected, indicating that the index of refraction was greater than 1. Analysis of the COMET experiments showed that the bound electrons have a large contribution to the index of refraction with the opposite sign of the free electrons, and explained how the index of refraction is greater than 1 in some Al plasmas.[8]

The original analysis[8] of the index of refraction in partially ionized Al plasmas was done only for a single wavelength, 14.7 nm, which is the wavelength of the Ni-like Pd x-ray laser used in the experiments at LLNL.[5] It was done by combining individual calculations of the photoionization cross section and the dipole allowed lines for each ionization stage of Al. That analysis assumed that the entire population was in the ground state of each ionization stage and that there was no distribution of excited states. The analysis adjusted the theoretical calculations so the lines and photoionization edges matched the positions measured in the experiments. It became clear that we needed the capability to calculate the index of refraction for arbitrary plasma at any wavelength.

For decades the INFERNO average atom code[9] has been used to calculate the distribution of levels and the absorption coefficient for plasmas of a given tempera-

J. Nilsen (jnilsen@llnl.gov) is with the Lawrence Livermore National Laboratory, Livermore, California 94551. W. R. Johnson is with the University of Notre Dame, Notre Dame, Indiana 46556.

Received 17 February 2005; revised manuscript received 28 April 2005; accepted 6 May 2005.

0003-6935/05/347295-07$15.00/0

ture and density. Using a modified version of this code,[10] we are now able to calculate the index of refraction for a wide range of plasma conditions. In this work we present the results for calculations of C, Al, Ti, and Pd plasmas that vary from singly to many times ionized. The index of refraction is calculated for photon energies from 0 to 100 eV (12.4 nm). These calculations enable us to understand under what plasma conditions the free-electron approximation is valid and provides an estimate of the bound-electron contribution.

It is important to note that bound electrons are the dominant contribution to the index of refraction in solid materials at standard temperature and pressure. This is the basis for conventional glass optics in the visible and normal-incidence multilayer optics in the x-ray regime.[11,12] For ionized plasmas, the plasma physics community generally ignores the contribution from bound electrons and relies on the approximation that the index of refraction of plasmas is due solely to the free electrons. In this paper we attempt to bridge the gap between these regimes by calculating what happens as one makes the transition between neutral room-temperature materials and hot ionized plasmas. We will show that the contribution from bound electrons to the index of refraction can be important over a large regime of partially ionized plasmas and that the influence of the bound electrons extends far from the absorption edges and resonance lines. Resonance lines can affect the index of refraction at photon energies that are located orders of magnitude further removed from the line than the width of the line.

For diagnostics, such as interferometers that depend on the index of refraction, it is important to understand the contribution from the bound electrons in order to properly analyze experiments.

## 2. Kubo–Greenwood Technique for Calculating the Index of Refraction

For many years the average atom technique incorporated in the INFERNO code[9] has been used to calculate the ionization conditions and absorption spectrum of plasmas under a wide variety of conditions. For finite temperatures and densities, the INFERNO code calculates a statistical population for occupation of one-electron Dirac orbitals in the plasma. In this work, we use a nonrelativistic version of INFERNO to calculate bound and continuum orbitals and the corresponding self-consistent potential. Applying linear-response theory to the average atom leads to an average-atom version of the Kubo–Greenwood equation[13,14] for the frequency-dependent conductivity of the plasma. Molecular-orbital versions of the Kubo–Greenwood formula have also been used in recent years to study the conductivity of Al plasmas.[15,16] The conductivity is proportional to the imaginary part of the complex dielectric function. Using the Kramers–Kronig[17] dispersion relation, the real part of the dielectric function is determined from its imaginary part. Knowing the complex dielectric function, the optical properties of the plasma, such as its index of refraction and absorption coefficients, are completely determined. The details of the Kubo–Greenwood formula applied to the average atom model are described in detail in a separate paper.[10]

## 3. Traditional Analysis of Interferometer Experiments

The usual formula for the index of refraction of a plasma due to free electrons is $n = (1 - N_{\mathrm{elec}}/N_{\mathrm{crit}})^{1/2}$, where $N_{\mathrm{elec}}$ is the electron density of the plasma and $N_{\mathrm{crit}}$ is the plasma critical density. At wavelength $\lambda$, $N_{\mathrm{crit}} = \pi/(r_0\lambda^2)$, where $r_0 = 2.818 \times 10^{-13}$ cm is the classical electron radius.[2] Since experiments typically measure an electron density that is much less than the critical density, the formula above is approximated by $n = 1 - (N_{\mathrm{elec}}/2N_{\mathrm{crit}})$. In a typical interferometer experiment[3–7] that probes a uniform plasma of length $L$ using a source with wavelength $\lambda$ the number of fringe shifts is equal to $(1 - n)L/\lambda$. This assumes that one arm of the interferometer propagates through vacuum and that one compares the fringe shifts against a set of reference fringes in the absence of any plasma. With the above approximation for $n$, the number of fringe shifts equals $(N_{\mathrm{elec}}L)/(2\lambda N_{\mathrm{crit}})$. The experimental analysis is done by simply counting how far the fringes have shifted compared with the reference fringes and converting this into electron density. For the 14.7 nm Pd x-ray laser the number of fringe shifts in the interferometer is $(N_{\mathrm{elec}}L)/(1.5 \times 10^{19}\ \mathrm{cm}^{-2})$ and the critical density is $5.17 \times 10^{24}\ \mathrm{cm}^{-3}$.

## 4. Analysis of Al Plasmas

Since the anomalous index of refraction results were first observed in Al plasmas[4,5] using x-ray laser interferometers, we utilize our new average atom code to analyze some Al plasmas. To simplify the analysis, the calculations using the average atom code were done for different temperatures but with a constant ion density of $10^{20}\ \mathrm{cm}^{-3}$. Since the fringe shifts are proportional to $(1 - n)$ we compare the ratio of $(1 - n)/(1 - n_{\mathrm{free}})$, where $n_{\mathrm{free}}$ is the index of refraction due only to the free-electron contribution. If only the free electrons contribute to the index of refraction this ratio equals 1 and the traditional analysis is valid. Otherwise this ratio represents the ratio of the measured electron density to the actual electron density when one analyzes the interferometer experiment the traditional way, assuming that only free electrons contribute to the index of refraction.

Even though the calculations are done for a single-ion density, the ratio normalizes away the actual density and we expect the analysis to be valid over a wider range of densities. One limitation of the calculations is that the average atom code assumes that the electron, ion, and radiation temperatures are all equal and that the plasma's ionization is in local thermodynamic equilibrium (LTE). For a dynamic plasma that is not in LTE we can first calculate the ionization condition ($Z^*$) of the plasma with a plasma kinetics code. We can then find an equivalent ionization condition ($Z^*$) with the average atom code and calculate the index of refraction for that condition

even though the temperatures may be different for the two codes. Since most of the absorption processes are associated with population in the ground state of the individual ionization stages, matching the $Z^*$ will give the best result. $Z^*$ is the ionization condition of the plasma such that $Z^* = 1$ means the average ion is singly ionized, 2 means double ionized, etc.

Figure 1(a) shows the ratio $(1 - n)/(1 - n_{\text{free}})$ versus photon energy for an Al plasma with a temperature of 2 eV and corresponding $Z^* = 0.92$, which means that the average ion is almost singly ionized. The dotted lines are plotted at ratios of 0 and 1 as visual aids. One immediately notices that the ratio is negative from 75 to 100 eV with typical values ranging from $-1$ to $-4$. This means the index of refraction of the plasmas is greater than 1. At 84.46 eV, which is the energy of the Pd x-ray laser (14.68 nm), the ratio is $-2.8$. In the detailed analysis of Al done in Ref. 8, the ratio for singly ionized Al was $-4.2$. In both calculations a Mach–Zehnder or Fresnel bimirror interferometer, as used in Refs. 4 and 5, would observe that the fringes bend in the opposite direction and by a larger distance than would be expected for the electron density being measured. Looking at lower energies, such as the 26.4 eV (46.9 nm) of the Ne-like Ar x-ray laser[6] that has been used for many interferometer experiments, the ratio is 2.6. An interferometer built at this wavelength could measure an electron density that is 2.6 times larger than the actual density. It is striking that the ratio crosses one but differs significantly from one over most of this energy range. Even at low energies, such as 4.68 eV, which is the energy of the fourth harmonic of the 1.06 μm Nd laser, the ratio is predicted to be $-3.0$.

It is important to recognize that an average atom calculation has an average value for the position of the absorption lines and edges based on $Z^*$, which can have noninteger values. This introduces uncertainty in the calculation, especially in regions of rapid change. However, slight shifts in the calculation to align the calculated and measured lines in the region of interest can greatly reduce the uncertainty in the calculations. The calculations are an invaluable first step in understanding the validity of the experiments and the potential corrections needed.

Figure 1(b) plots the ratio versus photon energy for an Al plasma with a temperature of 5 eV and $Z^* = 2.12$, which means it is slightly more than doubly ionized, on average. At energies below 40 eV the ratio is close to unity. For example, the ratio is 1.15 at the 26.4 eV energy of the Ne-like Ar x-ray laser and approaches unity for this laser as we continue to ionize the Al plasma. However, near 84 eV the ratio has very strong oscillations because of the presence of strong lines. The structure is sufficiently complex and highlights how a quantitative analysis in this oscillating region needs to know the exact positions of the absorption lines accurately. However, the calculations will be accurate away from the strong oscillations.

In Fig. 1(c) we plot the ratio for a 10 eV Al plasma with $Z^* = 2.88$, which is an almost triply ionized

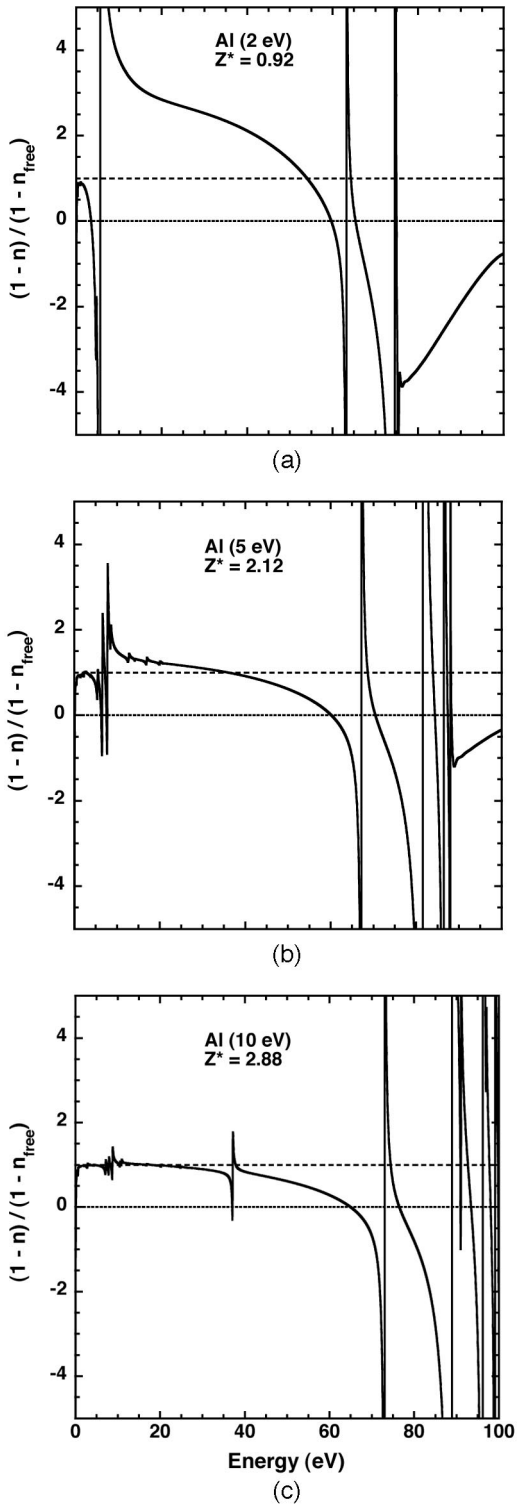


Fig. 1. Ratio $(1 - n)/(1 - n_{\text{free}})$ versus photon energy for Al plasmas with temperatures of (a) 2, (b) 5, and (c) 10 eV. The corresponding ionization is $Z^* = 0.92$, 2.12 and 2.88, respectively. The ion density is $10^{20}$ cm$^{-3}$. The dotted lines at ratios of 0 and 1 are visual aids.

Ne-like Al. In Ne-like Al the strong $3s$–$2p$ resonance lines are centered at 16.08 nm or 77.07 eV.[18] This figure shows a strong feature at 73.0 eV due to these

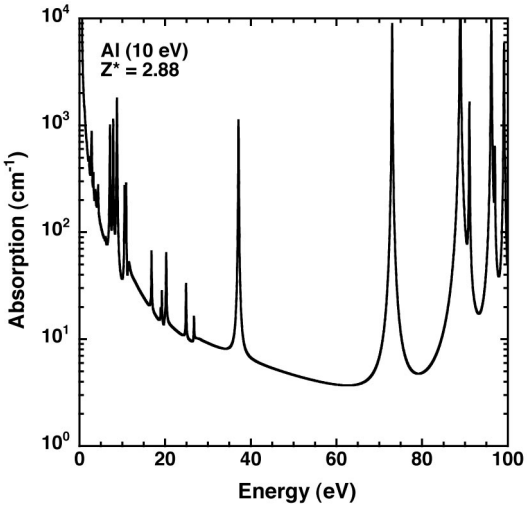


Fig. 2. Absorption coefficient versus photon energy for an Al plasma with a temperature of 10 eV. The ion density is $10^{20}$ cm$^{-3}$.

absorption lines. One can obtain a more accurate estimate of the ratio by shifting this feature a few eV to agree with the experimentally observed values of the lines. In Fig. 1(c) the ratio at 84.46 eV is $-2.4$ but reduces to $-0.9$ if one shifts the spectrum by 4.07 eV to match the position of the Ne-like resonance line. Reference 8 predicted a ratio of $-0.6$ for triply ionized Al at this photon energy. All three analyses predict that the ratio is negative and that the index of refraction is greater than one. This is consistent with the fringe lines in an interferometer experiment bending in the opposite direction than expected.

Another important plasma property to consider is the absorption coefficient of the plasma since the x rays or optical photons need to penetrate the plasma to be useful for interferometer measurements. Figure 2 shows the absorption coefficient versus photon energy for an Al plasma of 10 eV temperature with an ion density of $10^{20}$ cm$^{-3}$. For the region between 75 and 85 eV, and also between 40 and 70 eV, the absorption coefficient is less than 10 cm$^{-1}$. Since a typical interferometer experiment uses a 0.1 cm long plasma, this means the plasma will be optically thin to the x rays. Again, keep in mind that the spectra needs to be shifted approximately 5 eV to higher energy to agree with the experiments, so even the 89 eV Ag x-ray laser used in the experiments in Ref. 4 would have low absorption under these conditions.

As we continue to ionize the Al plasma Fig. 3(a) shows the ratio $(1 - n)/(1 - n_{\text{free}})$ versus photon energy for a 20 eV Al plasma with $Z^* = 4.64$. Much of the complicated structure disappears at energies near 84 eV but the ratio is still only 0.6 and is in good agreement with the value of 0.5 that one interpolates from Ref. 8. In this case the fringes would bend in the expected direction in an interferometer experiment but the measured value of the electron density would be lower by 40–50%.

Finally, Fig. 3(b) shows the ratio for a 40 eV Al plasma with $Z^* = 7.64$. While the ratio is not exactly

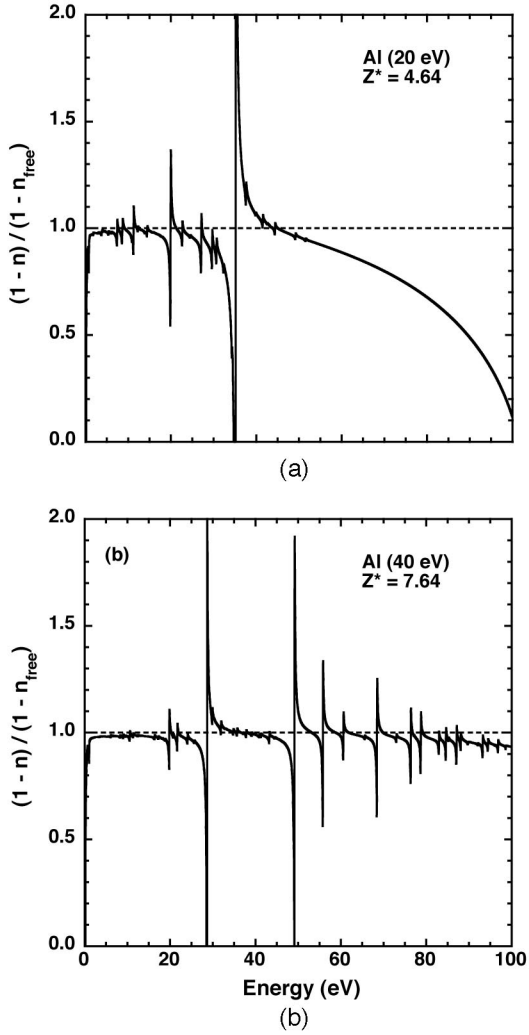


Fig. 3. Ratio $(1 - n)/(1 - n_{\text{free}})$ versus photon energy for Al plasmas with temperatures of (a) 20 and (b) 40 eV. The corresponding ionization is $Z^* = 4.64$ and 7.64, respectively. The ion density is $10^{20}$ cm$^{-3}$. The dotted line at a ratio of 1 is a visual aid.

one, it is within 10% of unity for most of the figure with the exception of some weak resonances. One had to ionize almost 8 of the 13 electrons from Al to approach the free-electron approximation for the index of refraction. This is the same conclusion reached in Ref. 8. The Al experiments highlight how the traditional equation for the index of refraction in plasmas is not valid over a large range of plasma conditions and photon energies. At optical photon energies near a few eV the free-electron approximation to the index for Al plasmas appears to be valid except for the singly ionized case.

### 5. Analysis of Other Plasmas Using Carbon, Titanium, or Palladium

Since plastics and other materials containing carbon are commonly used in experiments we looked at the index of refraction in carbon plasmas. Again we fix the ion density of the plasma at $10^{20}$ cm$^{-3}$. Figures 4 and 5 plot the ratio $(1 - n)/(1 - n_{\text{free}})$ versus photon energy for C

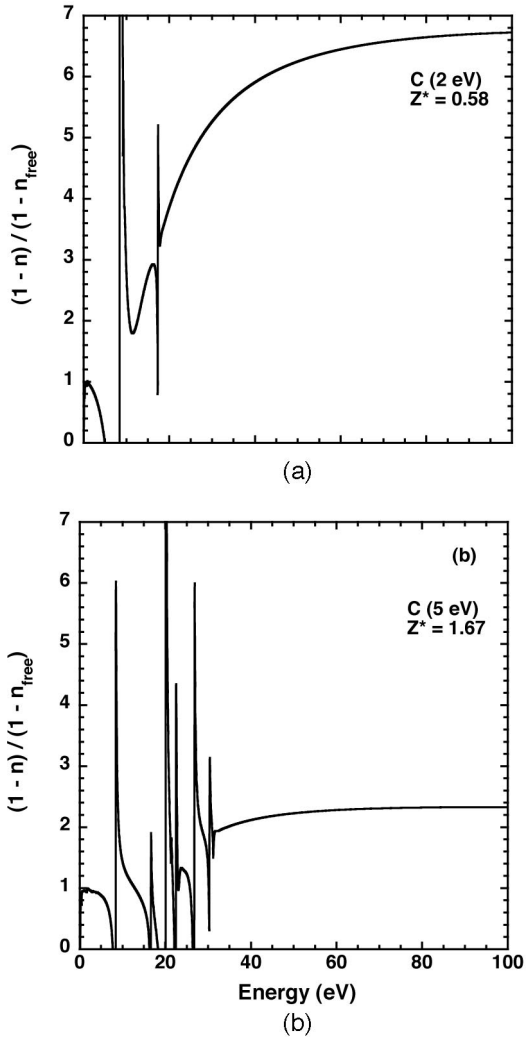


Fig. 4. Ratio $(1 - n)/(1 - n_{\text{free}})$ versus photon energy for C plasmas with temperatures of (a) 2 and 5 eV. The corresponding ionization $Z^* = 0.58$ and 1.67, respectively. The ion density is $10^{20}$ cm$^{-3}$.

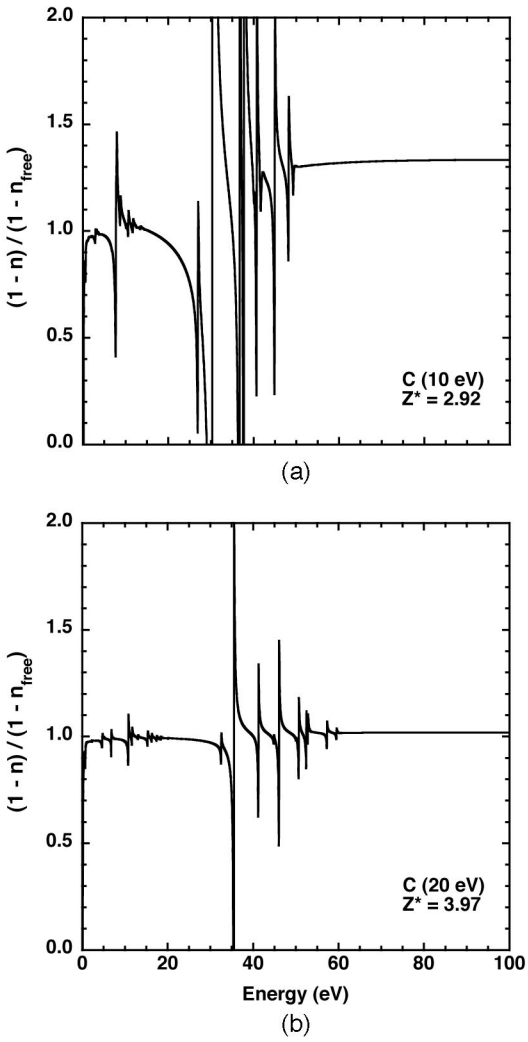


Fig. 5. Ratio $(1 - n)/(1 - n_{\text{free}})$ versus photon energy for C plasmas with temperatures of (a) 10 and (b) 20 eV. The corresponding ionization $Z^* = 2.92$ and 3.97, respectively. The ion density is $10^{20}$ cm$^{-3}$.

plasmas with temperatures ranging from 2 to 20 eV and the corresponding $Z^*$ ranging from 0.58 to 3.97. One notices that the figures are complicated for photon energies below 50 eV. Focusing on the 84.46 eV energy of the Pd x-ray laser used in the interferometer experiments[5] at LLNL, one observes that the ratio can be much larger than unity at low ionization states of C. For the 2 eV plasma the ratio is 6.7 at this photon energy. This would result in an experiment that greatly overestimates the electron density of the plasma. The fringes would bend in the expected direction, however, they would bend almost seven times more than expected for the actual electron density. Even at 10 eV, where the plasma is almost triply ionized, the ratio is 1.3 from 60 to 100 eV so experiments done with these energies would overestimate the electron density by 30%. The C plasma at 20 eV, which is almost four times ionized, has a ratio of 1.02 for energies above 60 eV and is close to 1 over the whole range with a few small oscillations. The C plasma needs to be ionized down to the $K$ shell before the free-electron contribution dominates the index of refraction in this energy range. Keep in mind that if we look at higher photon energies near the $K$ edges the ratio will again deviate substantially from 1.

Ti plasmas have been studied for many reasons including for their use as x-ray lasers.[19] Figure 6(a) shows the ratio $(1 - n)/(1 - n_{\text{free}})$ versus photon energy for several Ti plasmas with temperatures of 5 and 40 eV. Again we fix the ion density of the plasma at $10^{20}$ cm$^{-3}$. At 5 eV the plasma is approximately doubly ionized and the ratio is approximately 4 over the 80–100 eV photon range, meaning an interferometer experiment using this photon energy would overestimate the electron density by a factor of 4. One needs to be almost ten times ionized, as shown for the 40 eV curve, to have the ratio approach one over most of the plot. Even then there is a resonance near 100 eV that significantly changes the results if you are close enough to this weak resonance. Figure

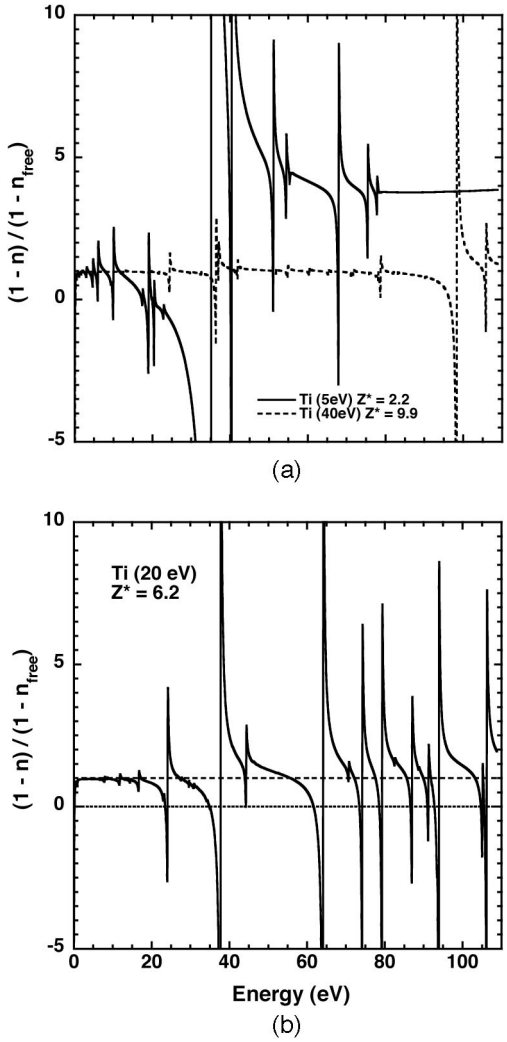


Fig. 6. (a) Ratio $(1 - n)/(1 - n_{\text{free}})$ versus photon energy for 5 and 40 eV Ti plasmas with $Z^* = 2.2$ and 9.9, respectively. (b) Ratio for Ti plasma with a temperature of 20 eV and $Z^* = 6.2$. The dotted lines at ratios of 0 and 1 are visual aids. The ion density is $10^{20}$ cm$^{-3}$ for all the Ti plasmas.

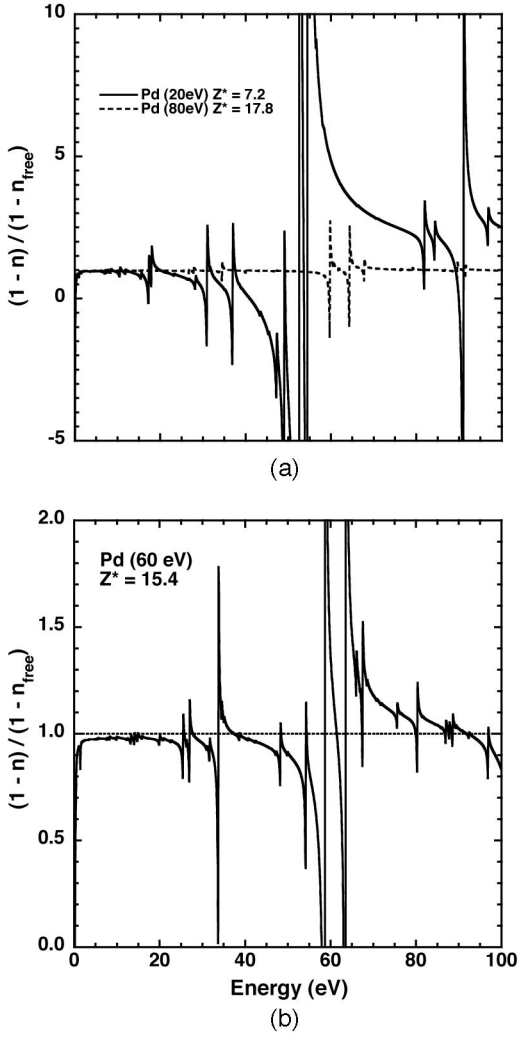


Fig. 7. (a) Ratio $(1 - n)/(1 - n_{\text{free}})$ versus photon energy for 20 and 80 eV Pd plasmas with $Z^* = 7.2$ and 17.8, respectively. (b) Ratio for Pd plasma with a temperature of 60 eV and $Z^* = 15.4$. The dotted line at a ratio of 1 is a visual aid. The ion density is $10^{20}$ cm$^{-3}$ for all the Pd plasmas.

6(b) shows the ratio for a 20 eV Ti plasma with $Z^* = 6.2$. A dotted line is shown with the value of 1 as a visual aid. The figure is rich in structure and shows how complicated it is to analyze a Ti plasma under these conditions.

Pd has been used successfully as an x-ray laser for many years. Recently, experiments[20] have been done to measure the plasma conditions of the Ni-like Pd x-ray laser just prior to lasing. The Pd laser is created by first using a prepulse to illuminate a solid target. The target heats and expands to create a plasma at the correct density and ionization to lase. The prepulse is followed by a short, high-intensity pulse that rapidly heats the plasma to lasing conditions and ionizes regions of the plasma that are slightly underionized to create the 18 times ionized Ni-like Pd plasma. Figure 7(a) shows the ratio $(1 - n)/(1 - n_{\text{free}})$ versus photon energy for Pd plasmas at 20 and 80 eV with $Z^* = 7.2$ and 17.8, respectively. Again we fix the ion density of the plasma at $10^{20}$ cm$^{-3}$. At 84.46 eV the ratio is 2.6 for the 20 eV plasma but is 1.0 for the 80 eV plasma. This figure shows how even seven times ionized Pd has a large contribution from the bound electrons to the index of refraction. By the time the plasma is near Ni-like Pd the ratio approaches 1 over this entire energy range except for some small resonances. Since the Pd plasma may be a few times less ionized than Ni-like in the interferometer experiments[20] that measure the condition of the Pd plasma created by the prepulse, Fig. 7(b) shows the ratio for a 60 eV Pd plasma with $Z^* = 15.4$. A dotted line at 1 is plotted as a visual aid. At 84.46 eV the ratio is 1.05 so the interferometer experiments could have a small overestimate of approximately 5% if the plasma is only 15 times ionized. This is an example of using the average atom code to validate that the interferometer experiments are being done in a regime of validity for the free-electron approximation to the index of refraction. This also

enables us to estimate the contribution from the bound electrons.

## 6. Conclusions

We have shown how the bound electrons can make a large contribution to the index of refraction in a plasma over the photon range from the optical up to 100 eV (12 nm) soft x rays. For decades the analysis of plasma diagnostics, such as interferometers, have relied on the approximation that the index of refraction of a plasma is due solely to the free electrons. This makes the index of refraction less than 1 and is also an essential assumption used in energy deposition in the plasma and for photon transport calculations. Recent measurements of Al plasmas using x-ray laser interferometers observed anomalous results with the index of refraction being larger than 1. The analysis of the Al plasmas show that the bound electrons can have the dominant contribution to the index of refraction from both absorption edges and lines. It is well known that a strong resonance line can cause anomalous results near the wings of an absorption line, but this work shows that the effects from the lines can extend to energies that are orders of magnitude further removed from the line than the width of the line. Similar long-range effects are shown for the absorption edges.

Utilizing, to the best of our knowledge, a new average atom code, we calculate the index of refraction in C, Al, Ti, and Pd plasmas and show many conditions over which the bound-electron contribution dominates the free electrons as we explore photon energies from the optical to 100 eV (12 nm) soft x rays. During the next decade x-ray free-electron lasers and other sources will be available to probe a wider variety of plasmas at higher densities and shorter wavelengths so it will be even more essential to understand the index of refraction in plasmas.

The authors thank K. T. Cheng, who made valuable suggestions in the process of preparing this work. This work was performed under the auspices of the U.S. Department of Energy by the University of California Lawrence Livermore National Laboratory under Contract W-7405-ENG-48. This research was also sponsored by the National Nuclear Security Administration under the Stewardship Science Academic Alliances program through U.S. Department of Energy Research grant DE-FG03-02NA00062. W. R. Johnson was supported in part by National Science Foundation grant PHY-0139928.

## References

1. G. J. Tallents, "Interferometry and refraction measurements in plasmas of elliptical cross section," J. Phys. D **17,** 721–732 (1984).
2. H. R. Griem, *Principles of Plasma Spectroscopy* (Cambridge University Press, 1997), p. 9.
3. L. B. Da Silva, T. W. Barbee, Jr., R. Cauble, P. Celliers, D. Ciarlo, S. Libby, R. A. London, D. Matthews, S. Mrowka, J. C. Moreno, D. Ress, J. E. Trebes, A. S. Wan, and F. Weber, "Electron-density measurements of high-density plasmas using soft x-ray laser interferometry," Phys. Rev. Lett. **74,** 3991–3994 (1995).
4. H. Tang, O. Guilbaud, G. Jamelot, D. Ros, A. Klisnick, D. Joyeux, D. Phalippou, M. Kado, M. Nishikino, M. Kishimoto, K. Sukegawa, M. Ishino, K. Nagashima, and H. Daido, "Diagnostics of laser-induced plasma with soft x-ray (13.9 nm) bimirror interference microscopy," Appl. Phys. B **78,** 975–977 (2004).
5. J. Filevich, J. J. Rocca, M. C. Marconi, S. J. Moon, J. Nilsen, J. H. Scofield, J. Dunn, R. F. Smith, R. Keenan, J. R. Hunter, and V. N. Shlyaptsev, "Observation of a multiply ionized plasma with index of refraction greater than one," Phys. Rev. Lett. **94,** 035005 (2004).
6. J. Filevich, K. Kanizay, M. C. Marconi, J. L. A. Chilla, and J. J. Rocca, "Dense plasma diagnostics with an amplitude-division soft x-ray laser interferometer based on diffraction gratings," Opt. Lett. **25,** 356–358 (2000).
7. D. Descamps, C. Lyngå, J. Norin, A. L'Hullier, C.-G. Wahlström, J.-F. Hergott, H. Merdji, P. Salières, M. Bellini, and T. W. Hänsch, "Extreme ultraviolet interferometry measurements with high-order harmonics," Opt. Lett. **25,** 135–137 (2000).
8. J. Nilsen and J. H. Scofield, Plasmas with an index of refraction greater than one," Opt. Lett. **29,** 2677–2679 (2004).
9. D. A. Liberman, "Inferno: A better model of atoms in dense plasmas," J. Quant. Spectrosc. Radiat. Transfer **27,** 335–399 (1982).
10. W. R. Johnson, C. Guet, and G. F. Bertsch, "Optical properties of plasmas based on an average-atom model," J. Quant. Spectrosc. Radiat. Transf. (to be published).
11. M. Born and E. Wolf, *Principles of Optics* (Pergamon, 1980), pp. 90–98.
12. B. L. Henke, E. M. Gullikson, and J. C. Davis, "X-ray interactions: photoabsorption, scattering, transmission, and reflection at $E = 50–30{,}000$ eV, $Z = 1–92$," At. Data Nucl. Data Tables **54,** 181–342 (1993).
13. D. A. Greenwood, "The Boltzmann equation in the theory of electrical conduction in metals," Proc. Phys. Soc. **71,** 585–596 (1958).
14. R. Kubo, "Statistical-mechanical theory of irreversible processes. I. General theory and simple applications to magnetic and conduction problems," J. Phys. Soc. Jpn. **12,** 570–586 (1957).
15. M. P. Desjarlais, J. D. Kress, and L. A. Collins, "Electrical conductivity for warm dense aluminum plasmas and liquids," Phys. Rev. E **66,** 025401 (2002).
16. V. Recoules, P. Renaudin, J. Clèouin, P. Noiret, and G. Zèrah, "Electrical conductivity of hot expanded aluminum: experimental measurements and *ab initio* calculations," Phys. Rev. E **66,** 056412 (2002).
17. L. D. Landau and E. M. Lifshitz, *Electrodynamics of Continuous Media* (Pergamon, 1984), pp. 280–283.
18. R. L. Kelley, "Atomic and ionic spectrum lines below 2000 angstroms: hydrogen through krypton," J. Phys. Chem. Ref. Data Suppl. 1, **16** (American Institute of Physics, 1987), p. 223.
19. J. Nilsen, B. J. MacGowan, L. B. Da Silva, and J. C. Moreno, Prepulse technique for producing low-$Z$ Ne-like x-ray lasers," Phys. Rev. A **48,** 4682–4685 (1993).
20. R. F. Smith, J. Dunn, J. Filevich, S. Moon, J. Nilsen, R. Keenan, V. N. Shlyaptsev, J. J. Rocca, J. R. Hunter, and M. C. Marconi, "Plasma conditions for improved energy coupling into the gain region of the Ni-like Pd transient collisional x-ray laser," Phys. Rev. E **72,** 036404 (2005).